Majoron Dark Matter and Neutrino Masses in the Type 1 Seesaw Mechanism

MoCa 2020

Gustavo Ardila [1], Nathalia Cardona [2], Andres Florez [2], Werner Rodejohann [3], Nicolas Vergara [2]

[1] Universität Heidelberg, [2] Universidad de los Andes, [3] Max Planck Institut für Kernphysik

October 7, 2020

Overview

- Standard Model (SM) is not complete. It cannot explain phenomena like Dark Matter (DM) or neutrino masses.
- Homestake experiment detected neutrino data showed a discrepancy between the expected flux of solar neutrinos and the experimental data.
- Not enough statistics
- Later: Kamiokande and SNO confirmed this discrepancy $\rightarrow$ Muon neutrinos were detected.
- Neutrinos are oscillating between flavor states with probability

$$P(e \rightarrow \mu) = \sin^2(2\theta_{mix}) \sin^2\left(\frac{1.27\Delta m^2 L}{E}\right) \tag{1}$$

- Simple solution: introduce 3 Right-Handed (RH) singlets, one for each lepton flavor. Dirac masses can be generated via SM Yukawas

$$-\mathcal{L} \supset \Gamma^{\nu}_{ij} \bar{\ell}^{i}_{L} \tilde{\phi} \nu^{j}_{R}; \quad i = e, \mu, \tau; \quad \tilde{\phi} = i\tau_2 \phi^* \tag{2}$$

- After electroweak SSB one obtains mass terms and couplings with the SM Higgs

$$-\mathcal{L} \supset \frac{1}{\sqrt{2}} f^{\nu}_{ij} v \bar{\nu}_L \nu_R + \frac{1}{\sqrt{2}} f^{\nu}_{ij} \bar{\nu}_L h \nu_R \tag{3}$$

$$= M^{D}_{ij} \bar{\nu}_L \nu_R + \frac{1}{v} M^{D}_{ij} \bar{\nu}_L h \nu_R \tag{4}$$

- Masses can be easily obtained. Why are the experimental mass values so small?

- One can explain the small neutrino masses by introducing 3 Majorana neutrinos with mass term

$$-\mathcal{L} \supset \frac{1}{2}\bar{\nu}_L^c M_M \nu_R + h.c \tag{5}$$

- Note that mass term breaks lepton number by two units as L(ν_R)=L($\bar{\nu}_L^c$)=1.
- Lepton number violation can be used to explained baryon assymetry in the universe through leptogenesis. Can be promoted to approximate symmetry at a "classical" level.
- General mass Lagrangian considers both Dirac and Majorana masses

$$-\mathcal{L} \supset \frac{1}{2}\bar{\nu}_L^c M_N \nu_R + h.c; \quad \nu_R = (\nu_L^c, \nu_R) \tag{6}$$

- Mass matrix is non diagonal

$$M_N = \begin{pmatrix} 0 & M_D \\ M_D^T & M_M \end{pmatrix} \tag{7}$$

Weak eigenstates$\neq$ mass eigenstates

- Diagonalize via orthogonal matrix V

$$M_d = \mathrm{diag}(m_1, \cdots, m_6) = V^T M_N V \tag{8}$$

- M_d can be obtained from the block diagonal matrix

$$M_N' = \mathrm{diag}(\lambda_1, \lambda_2); \quad \lambda_{1,2} = \frac{1}{2}[M_M \pm \sqrt{M_M^2 + 4M_D^T M_D}] \tag{9}$$

- Reduce the squared root by considering that M_M eigenvalues are larger than those of M_D

$$M'_N = \begin{pmatrix} M_M & 0 \\ 0 & -M_M^{-1} M_D^T M_D \end{pmatrix} \tag{10}$$

- Easier understanding: Consider just one family, then

$$M'_N = M_d = \begin{pmatrix} m_m & 0 \\ 0 & \frac{m_D^2}{m_m} \end{pmatrix} \tag{11}$$

- Second eigenvalue becomes small if one of the values is large enough $\rightarrow$ Seesaw scale $O(TeV)$.

- Type 1 Seesaw explains why measured mass values are so small. However, L gets broken by two units and M_M is put by hand.
- One can then promote L, or B-L, to an approximate global symmetry that becomes spontaneously broken at the Seesaw scale.
- Introduce scalar singlet φ with potential

$$V(\phi) = m_\varphi^2 \varphi^\dagger \varphi + \frac{\lambda_\varphi}{4}(\varphi^\dagger \varphi)^2 + V(\phi, \varphi) \tag{12}$$

- Hence, one can generate Majorana masses through Yukawa couplings

$$-\mathcal{L} \supset \frac{1}{2} y_{ij} \bar{\nu}_L^{c,i} \varphi \nu_R^j + h.c \tag{13}$$

- It is possible to parametrize φ around the new VEV as

$$\varphi = \frac{1}{\sqrt{2}}(f + A + iJ) \tag{14}$$

- Goldstone theorem $\rightarrow$ J gets massive. Referred to as the Majoron.
- If Seesaw scale = Peccei-Quinn scale, Majoron = Axion.

- After SSB, Majorana mass terms are obtained as well as Neutrino-Majoron interactions

$$-\mathcal{L} \supset \frac{1}{2}(M_M)_{ij}\bar{\nu}_L^{c,i}\nu_R^j + \frac{1}{2\sqrt{2}}y_{ij}\bar{\nu}_L^{c,i}A\nu_R^j + \frac{i}{2\sqrt{2}}y_{ij}\bar{\nu}_L^{c,i}J\nu_R^j \tag{15}$$

- Rewrite Neutrino-J couplings in terms of the masses

$$\mathcal{L}_J = \frac{im_N}{2f}\bar{\nu}_L^c J\nu_R + h.c \tag{16}$$

In terms of the three massive neutrino eigenstates

$$\mathcal{L}_J = \frac{im_N}{2f}\bar{n}_i J n_i + h.c \tag{17}$$

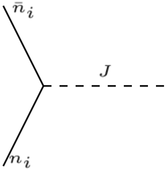

- Majoron production at the LHC has not been largely studied.
- Two fundamental production mechanisms were studied. First one: W mediated production of a Majoron.

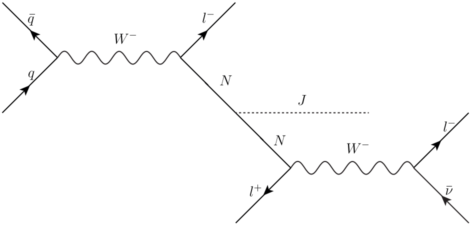

Figure: W mediated production of a J (W Channel)

- The other production mechanism emulates the signal from the $0\nu\beta\beta$ decay, and is obtained through indirect Vector Boson Fusion (VBF) processes

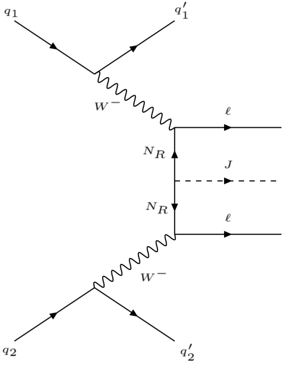

Figure: J production via VBF

- Scenarios with $\Delta m(N_1, J) = \Delta m(N_1, N_2) = \Delta m(N_2, N_3) = 100 GeV$ were considered with minimal $m(J) = 50 GeV$ due to QCD restrictions.
- 3 different mass points within the spectrum were generated

Table: Number of events produced for the analyzed mass spectra.

{m(J), m(N_e), m(N_μ), and m(N_τ)}	Number of events
{50, 150, 250, 350}	200.000
{200, 300, 400, 500}	200.000
{700, 800, 900, 1000}	200.000

Cross Section

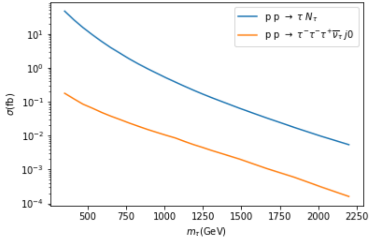

Figure: (Blue) Cross section as function of m(N_τ) considering production of stable neutrinos. (Yellow) Cross section considering Majoron radiation and non stable neutrinos.

- After analyzing both the cross section and the topology, basic selection criteria were considered, given CMS minimal reconstruction settings.

Criteria	Selections
$p_T(e)$	> 8 GeV
$p_T(\mu)$	> 5 GeV
$p_T(\tau)$	> 20 GeV
$\lvert\eta(e)\rvert, \lvert\eta(\mu)\rvert, \lvert\eta(\tau)\rvert$	< 2.4

Missing Transverse Energy distribution

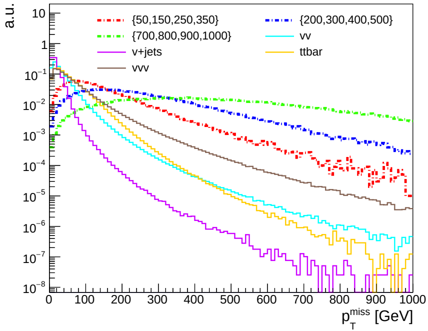

- Signal is characterized by large p_T^{miss} and p_T values, whereas backgrounds posses lower values given the SM topologies.

Transverse mass distribution

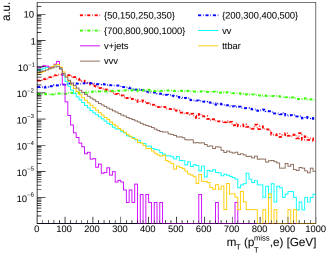

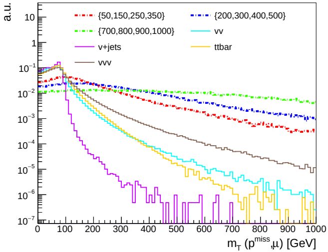

- The transverse mass (m_T) distribution was studied due to its relation with the p_T and p_T^{miss} variables. It is defined as

$$m_T = \sqrt{2p_T(\ell)p_T^{miss} \times (1 - cos(\Delta\phi(\ell, p_T^{miss})))} \qquad (18)$$

ST distribution

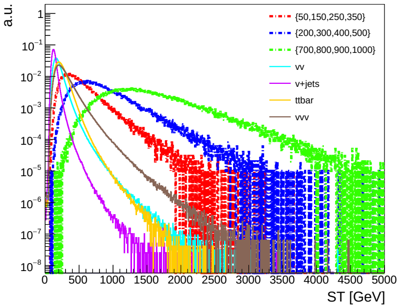

- Due to the large p_T and p_T^{miss} values of the signal. The ST distribution, which is defined as the scalar sum between the p_T and the p_T^{miss} was considered.
- This distribution gives a good separation between signal and background.

Central selection criteria

Table: Central Event Selection Criteria (II)

Criteria	Selections
p_T^{miss}	> 100 GeV
$N(b - jets)$	0
$p_T(\ell^{lead})$	> 50 GeV
$p_T(\ell^{other})$	> 20 GeV
$\Delta p_T(\ell^{lead}, \ell^{lowest})$	> 50 GeV

- After applying all both basic and central criteria, four different final states (channels) were considered $\{e, e, e\}$, $\{e, e, \mu\}$, $\{\mu, \mu, e\}$, $\{\mu, \mu, \mu\}$.

Cumulative efficiencies

Signals						
{m(J), m(N_1), m(N_2), m(N_3)}	ϵ_I	ϵ_{II}	ϵ_{III}	ϵ_{IV}	ϵ_V	ϵ_{VI}
{50, 150, 250, 350}	85.18	72.93	4.14	5.72	9.28	4.46
{200, 300, 400, 500}	95.52	86.51	8.22	5.69	6.89	8.59
{700, 800, 900, 1000}	99.01	92.53	12.13	4.86	4.89	11.26
Backgrounds						
Sample	ϵ_I	ϵ_{II}	ϵ_{III}	ϵ_{IV}	ϵ_V	ϵ_{VI}
www	41.56	29.44	4.47×10^{-2}	5.63×10^{-2}	3.84×10^{-2}	1.83×10^{-2}
zzw	43.36	28.94	6.81×10^{-2}	8.44×10^{-2}	15.29×10^{-2}	6.97×10^{-2}
zzz	41.41	26.62	4.15×10^{-2}	5.22×10^{-2}	7.13×10^{-2}	3.40×10^{-2}
wwz	47.51	32.52	8.76×10^{-2}	10.88×10^{-2}	15.58×10^{-2}	7.90×10^{-2}
wz	21.18	16.41	1.07×10^{-2}	1.44×10^{-2}	4.10×10^{-2}	2.85×10^{-2}
zz	20.00	15.66	2.13×10^{-3}	1.67×10^{-4}	8.26×10^{-3}	2.24×10^{-3}
ww	20.81	15.32	1.40×10^{-4}	4.00×10^{-5}	9.60×10^{-5}	2.32×10^{-4}
$t\bar{t}$	39.04	6.61	1.10×10^{-4}	1.73×10^{-4}	2.34×10^{-4}	1.60×10^{-4}
z+jets	2.79	2.54	5.40×10^{-6}	5.40×10^{-6}	-	5.4×10^{-6}
w+jets	3.89	2.99	-	-	-	-

- Cumulative efficiencies after the cuts. ϵ_I and ϵ_{II} are associated to the basic and central criteria, whereas $\epsilon_{III} - \epsilon_{VI}$ are the efficiencies of the $\{e, e, e\}$, $\{e, e, \mu\}$, $\{\mu, \mu, e\}$, $\{\mu, \mu, \mu\}$ channels after the first two cuts.

W Channel

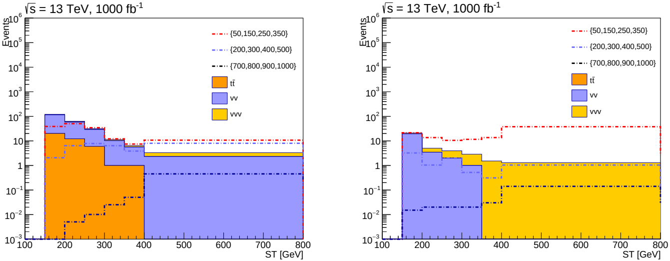

Figure: ST distribution for the expected number of events for $1000 fb^{-1}$ luminosity, for the most relevant backgrounds (stacked) and for three different signal samples, dashed lines overlaid on top of the backgrounds. The distribution on the left is for the eee channel and the distribution on the right is for the $\mu\mu\mu$ channel.

- Some background events fall on the high ST range which has large statistical uncertainties.
- Difference between plots due to the larger miss-identification rate of electrons, which is up to one order of magnitude higher than for muons

Cross sections

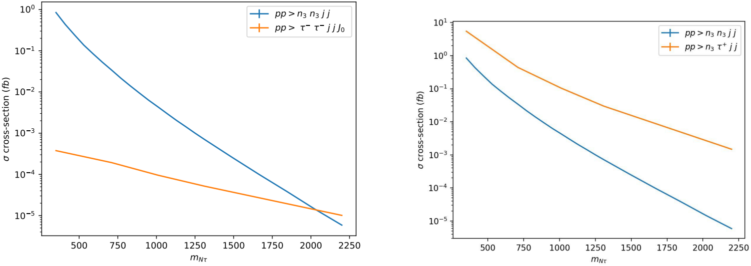

Figure: Left: (Blue) Cross section as function of m(N_τ) considering production of stable neutrinos. (Yellow) Cross section considering Majoron radiation and non stable neutrinos. Right: (Blue) Cross section as function of m(N_τ) considering production of stable neutrinos. (Yellow) Cross section considering Tau production with two jets and a stable neutrino.

η distribution

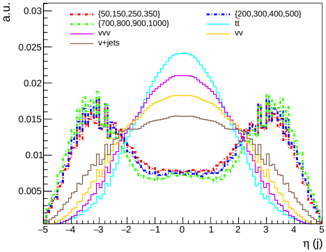

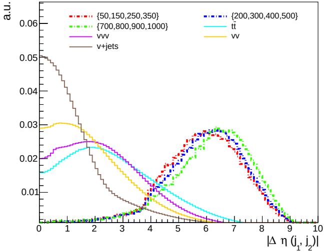

- From both distributions is noticeable that signal events follow the VBF topology, while background events locate on the barrel section of the detector.
- $\Delta\eta$ distribution shows the restriction made to the jets $|\Delta\eta(j_1, j_2) > 3.8$.

MET and ST distributions

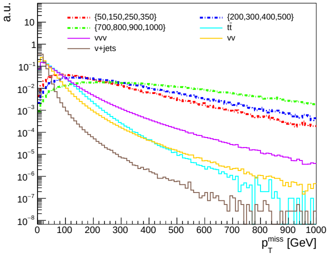

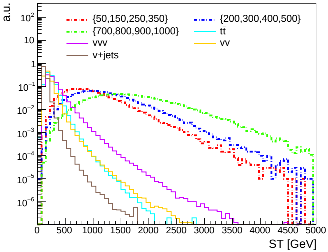

- p_T and p_T^{miss} values of the signal are larger than those of the background events.
- S_T distribution shows a good separation between signal and background. Can be used for data discrimination.

Topological and VBF selections

Table: Topological selections

Criteria	Selections
p_T^{miss}	> 150 GeV
$N(b - jets)$	0
$p_T(b - jets)$	> 30 GeV
$\lvert\eta(b - jets)\rvert$	< 2.5

Table: VBF selections

Criteria	Selections
$N(j)$	≥ 2
$p_T(j)$	> 30 GeV
$\lvert\eta(j)\rvert$	< 2.5
$\eta(j_1) \cdot \eta(j_2)$	< 0
$\lvert\Delta\eta(j_1, j_2)\rvert$	> 5.5

- After analyzing all the distributions, two sets of selection criteria were chosen. The topological criteria have been chosen to reduce as most QCD background as possible, whereas the VBF selections restrict the events to follow the desired topology.
- After these selections, two di-lepton channels were considered $\{e, e\}$, $\{\mu, \mu\}$ as well as two single lepton decays (e,μ)

Cummulative efficiencies

Signals						
{m(J), m(N_1), m(N_2), m(N_3)}	ϵ_I	ϵ_{II}	ϵ_{III}	ϵ_{IV}	ϵ_V	ϵ_{VI}
{200, 300, 400, 500}	65.985	30.128	4.852	4.476	4.215	9.354
{700, 800, 900, 1000}	82.519	38.423	7.028	5.162	6.887	11.311
{50, 150, 250, 350}	49.733	21.808	3.183	3.73	2.052	6.586

Backgrounds						
Sample	ϵ_I	ϵ_{II}	ϵ_{III}	ϵ_{IV}	ϵ_V	ϵ_{VI}
www	4.444	0.077	0.012	0.017	0.109×10^{-2}	0.17×10^{-2}
zzw	6.658	0.120	0.008	0.010	0.156×10^{-2}	0.24×10^{-2}
zzz	5.683	0.083	0.003	0.002	0.168×10^{-2}	0.26×10^{-2}
wwz	8.316	0.115	0.015	0.018	0.132×10^{-2}	0.16×10^{-2}
$t\bar{t}$	0.657	0.029	0.004	0.00639727	0.209×10^{-3}	0.382×10^{-3}
z+jets	0.102	0.001	1.621e-05	1.621e-05	5.400×10^{-3}	-
w+jets	0.051	0.001	0.133×10^{-3}	0.00019115	-	-
ww	0.799	0.014	2.096×10^{-3}	3.184×10^{-3}	5.6×10^{-5}	0.12×10^{-3}
zz	1.457	0.018	0.48×10^{-3}	0.39×10^{-3}	0.14×10^{-3}	0.22×10^{-3}
wz	1.251	0.024	1.431×10^{-3}	2.497×10^{-3}	4.061×10^{-5}	8.122×10^{-5}

- Cumulative efficiencies after the cuts. ϵ_I and ϵ_{II} are associated to the topological and VBF criteria. $\epsilon_{III} - \epsilon_{IV}$ are the efficiencies associated to single lepton (e,μ)production together with a stable heavy neutrino after the first two cuts. $\epsilon_V - \epsilon VI$ are associated to di-lepton production after ϵ_I and ϵ_{II}

Conclusions

- The considered two channels showed that Majoron production at the LHC can be achieved with large luminosity values at the LHC
- Selection criteria that were chosen for the two channels can be used for further studies.
- This study is a work in progress: Drell-Yan and Loop processes need to be considered.
- Non diagonal couplings?